Bondi-Hoyle Accretion in Dense Star Clusters: Implications for Stars, Disks, and Planets
Draft version: May 22, 2007

Henry B. Throop

Southwest Research Institute

1050 Walnut St, Ste 300, Boulder, CO 80302

throop@boulder.swri.edu

John Bally

Center for Astrophysics and Space Astronomy

University of Colorado, Boulder

UCB 389, Boulder, CO 80309-0389

Received _____; accepted _____

ABSTRACT

We investigate the Bondi-Hoyle accretion of gas from a GMC onto young star-disk systems in a cluster. This post-formation accretionary phase can continue for several Myr after young stars are born, until the gas is heated by massive stars and removed from the cluster, or when low-mass stars are ejected from the cluster. We perform N-body simulations of stars orbiting in young model clusters using 30, 500, and 3000 stars. We include the gravitational effects of stars and gas. The average mass accretion rate for a star dM/dt is proportional to M^2, consistent with observations of accretion in young stars. For solar mass stars, the accretion rate is approximately 5×10^{-9} $M_\odot$, and the total mass accreted is 0.05 $M_\odot$. The 1σ spread in accretion rates for stars of the same mass varies by a factor of 500, due to variations in stars's position and velocity. The mass accreted is insignificant compared to the star's mass, but it is comparable to or greater than the disk mass. The accretion flow is likely to pass through the disk, where it may significantly affect the planetesimal and planet-formation process, by increasing the amount of raw material available, and providing it over several Myr. We discuss a variety of implications of this process, including its effect on the formation of terrestrial and gas-giant planets, the migration of extrasolar planets, FU Ori outbursts, and metallicity variations between a star and its planets.

1. Introduction

Stars form from the collapse of molecular clouds. A typical giant molecular cloud (GMC) may have a mass $M \approx 10^3 - 10^4 M_\odot$. Self-gravity causes the cloud to begin to

collapse, and stars form in regions of local instability. A solar-mass star may take XX years to collapse, accrete mass, and begin fusion. Star formation in the cluster continues while the gas is unstable against collapse. It ceases when the remaining gas becomes stable again, either due to heating from high-mass stars, removal due to stellar winds, or depletion due to gas being used up by stellar formation.

Typical star-formation efficiency (SFE) in a cloud is 15% - 30%; that is, the majority of gas is not used to make stars, but ultimately gets removed from the cluster. The removal

In most GMCs, star formation stops soon after high-mass O and B stars form. These UV-bright stars heat and ionize the gas, inhibiting further collapse. The Orion Nebular Cluster (ONC) is one example of a large cluster in such a state. The Trapezium stars at its core are bathing the entire cluster and its gas in intense UV radiation. This radiation is sufficient to remove the cluster's remaining gas in $\ll 1$ Myr. In Orion, solar-mass stars are observed with ages of 1-2 Myr, significantly older than the 40,000 years or so that the nebula has shown evidence for being ionized by O and B stars.

After stars form, they orbit through the cluster, and through the remnants of the GMC. As stars pass orbit through the gas, material is accreted onto the stars by the Bondi-Hoyle accretion (Bondi 1952; Bondi & Hoyle 1944). BH accretion describes how material in a uniform gas cloud is gravitationally focused onto a moving point-mass. Ongoing accretion depends on the existence of relatively cold gas to accrete; accretion can slow as the gas speed (or stellar speed) increases, or if the gas becomes depleted. In OB associations the gas becomes ionized when high-mass stars turn on, ceasing BH accretion after perhaps $\sim 1 - 2$ Myr. In smaller, dark clouds, however, accretion may continue for several Myr.

Most previous studies of star clusters have differentiated between the star-formation process, and the subsequent evolution of stars (and formation of planets) within a cluster. The emphasis of our study is to investigate the environmental effects of a cluster's

unaccreted cold, dark gas cloud, on the evolution of the cluster's stars. This effect has not, to our knowledge, been studied before. We focus in particular on the effects around roughly solar-mass stars, since these are the stars most likely to be of interest to planet formation.

Bondi-Hoyle accretion has been suggested to explain observations of accretion in young stars, where the accretion rate onto the stars scales as the stellar mass, $\dot{M} \sim M_*^2$ (*e.g.* Padoan et al. 2005). Indeed, our results indicate that some of the observations of accretion could well be explained by this process. However, accretion onto stars has been observed in regions where BH accretion could *not* be happening at the observed rate (such as HII regions where the gas is too hot to efficiently accrete). We devote this paper not to explaining the $\dot{M} \sim M^2$ problem, but rather to exploring the consequences of Bondi-Hoyle accretion in systems in which it is most likely to be occurring. We discuss the M_*^2 problem in more detail in section 5.1.

In this paper, we perform N-body simulations of the motion of stars through three clusters, and calculate the gas accretion onto stars in these clusters. Section 2 describes the background and motivation. Section 3 describes our simulations, and Section 4 discusses our results. We discuss some possible implications for the formation of stars, disks, and planets in Section 5.

2. Background and Motivation

2.1. Bondi-Hoyle accretion

Bondi-Hoyle (BH) accretion describes how gas is accreted onto a small moving mass such as a star. It can be written as (Bondi 1952)

$$\dot{M}_{\rm BH} = \frac{4\pi\, G^2 M^2}{(v^2 + c_s^2)^{\frac{3}{2}}}\, v\, n\, m_h, \tag{1}$$

where G is the gravitational constant, n_h is the gas number density, m_h is the molecular mass, M is the stellar mass, v is the stellar speed, and c_s is the sound speed. It is convenient to define the Bondi-Hoyle radius, $R_{\rm BH}$, as

$$R_{\rm BH} = 2\frac{GM}{(v^2 + c_s^2)}. \tag{2}$$

A simple estimate allows us to gauge the importance of the process. For a typical dark cloud with $T = 50\,K$, we have $c_s = 1$ km s^{-1}. For $n = 10^4$ cm^{-3} and $v = 1$ km s^{-1}, we find that $\dot{M}_{\rm BH} \approx 2\ 10^{-8}\ M_\odot$ yr^{-1}, and $R_{\rm BH} \approx 1000$ AU. We can think of such a star gravitationally focusing and collecting material contained within a column of radiius 1000 AU. Because $R_{\rm BH}$ is substantially larger than the typical disk sizes of 10-100 AU in an HII region such as the Orion nebula (Bally et al. 1998), the BH accretion rate is $10^2 - 10^4$ times than simple physical 'sweep-up' of material by the disk.

The accretion rate in this example is 0.01 $M_\odot$per Myr, which is not enough to increase the star's mass significantly during the several Myr that accretion may operate. However, the accretion is most certainly significant compared to the mass of the disk, assuming a minimum-mass solar nebula (MMSN) disk of 0.01 $M_\odot$. As numerical experiments describe below show, much of this material probably does interact with the disk. The disk could receive several times its own mass deposited onto it within its first several Myr. This accretion may have significant impact on the disk, either by depositing new material, or disturbing the existing disk.

This process occurs after the star and disk are formed, but before the parent molecular cloud is dispersed. Depending on the local environment, this process may last $10^5 - 10^7$ yr. It is essentially a later, slower tail to the 'competitive accretion' that forms the stars from

the molecular cloud in the first place Bate & Bonnell (2005, *e.g.*). We denote this process 'post-formation accretion' (PFA).

In this paper we model the amount and rate of mass being deposited onto star-disk systems in a variety of young clusters.

BH accretion onto a star could be inhibited by sufficiently strong stellar winds. However, for the young solar-mass stars that we consider here, such winds are insignificant. Typical winds are descibed by $\dot{M}_{\rm wind} \lesssim 10^{-10}\ M_\odot\ {\rm yr}^{-1}$ and $v = 50$ km s^{-1} (REF). Even if the winds were strong, such winds and outflows come predominantly out the poles and high-latitude regions covering only a small fraction of a star's surface. For stars of $M > 10\ M_\odot$, (XXX) radiation pressure begins to be important, and can prevent BH mass accretion. Therefore, our results will consider only stars below this size.

Recent work by Krumholz et al. (2006) has simulated Bondi-Hoyle accretion from a turbulent medium. They find that the accretion rate generally decreases with increasing turbulence. In laminar regions like Taurusm the effect is likely to be mininal, while in large regions like Orion, they find greater turbulence is to decrease $\dot{M}_{\rm BH}$ by a factor of 5. We will discuss these implications further in Section 5.

3. Numerical simulations

The simple estimate in the previous section shows that PFA can be important. The actual accretion rates will vary spatially and temporally, depending on a star's velocity, mass, and the local gas density. In this paper we expand the simple calculation to compute the PFA rate over a range of stellar masses and cluster types. We use N-body simulations to determine the each star's dynamical and environmental history, and we compute the mass accretion based on this. variability of the rate

A variety of numerical codes to perform N-body gravitational simulations are available. We use the NBODY6 code (Aarseth 1999), which is a standard code for star cluster modeling. This is a sophisticated, Hermite-method integrator, and is very accurate in its handling of close approaches between stars. It allows for flexible control over initial input conditions, is fast, proven, and has a long heritage.

NBODY6 is particularly useful for us because it can model the dynamics of a cluster orbiting through a molecular cloud. The cloud is modeled as a gravitational Plummer potential of a given width and mass, which can decay at a specified rate. In this way, NBODY6 can treat the expansion of a cluster as the gas at its core disperses due to stellar winds and supernovae. This dispersal is smooth (not instantaneous), which is an improvement over many previous models (Adams et al. 2006, *e.g.*) that included gas dispersal, but only as a step-function. NBODY6 handles the gas's gravitational effect on the stars, but the stars themselves are assumed to have no effect on the gas. The gas's mass, shape, and evolution is controlled entirely by input parameters.

We perform our simulation in two discrete steps. First, we perform N-body simulations within the stellar cluster, and output the position and velocity of each star at fixed intervals of 2×10^4 yr. We then take our results, and calculate $\dot{M}_{\rm BH}$ at each step for each star, using Eq. [1].

We have made several simplifying assumptions. First, our simulation is not entirely self-consistent in that mass accreted onto stars is removed only as a general global process, and not locally in response to accretion. However, the gas mass lost to BH accretion by the end of the simulations is less than 1% of the original cloud mass, so ignoring this mass has no great effect. Second, because the sound speed is comparable to individual stellar velocities, local 'holes' will be filled quickly, making a local treatment unnecessary. A larger objection could be raised that the mass of individual stars in our simulation does not

increase in response to gas accretion. However, except for the largest stars ($M > 10\ M_{\odot}$), the mass accreted by a star is less than a few percent of the star's mass. This small increase makes insignificant change to a star's motion or its subsequent accretion.

For simplicity, we assume that all stars are fully-formed by $t = 0$. In reality, star formation is an on-going process that continues until the gas is depleted, heated, or no longer stable against collapse. Observations in the Orion nebula cluster (Hillenbrand 1997, *e.g.*) show that star formation has been occuring for most of the last 2 Myr. Therefore, our results should be regarded as upper limits for the total mass accreted by a star, because the youngest stars will have little opportunity for mass accretion before the gas is removed.

o Add here section about binaries?

o Add here section about BH accretion in a turbulent medium

3.1. Initial conditions and inputs

We have simulated the evolution of three different stellar clusters, with parameters listed in Table 1. The 'Small Cluster' model is a long-lived, small, dark cloud, similar to Taurus, with $N = 30$ stars spread over 0.5 pc and a GMC gas mass of 30 $M_{\odot}$. Masses are distributed using the initial mass function (IMF) of Kroupa et al. (1993). The minimum stellar mass is 0.1 $M_{\odot}$, and the mean is 0.5 $M_{\odot}$. Star formation efficiency (SFE) is the ratio $M_{\rm Stars} : (M_{\rm Stars} + M_{\rm Gas})$ and is 33%. The gas is retained entirely until $t = 5$ Myr, after which it is slowly lost to simulate the dispersal by stellar winds, diffusion, and cluster spreading.

Our 'Medium Cluster' models a region like IC348, with $N = 500$ stars. Accretion runs for 3 Myr, until the gas dispersion begins. Other parameters are the same. Finally, our 'Large Cluster' models the environment in a young version of the Orion Nebula Cluster (ONC), before OB stars have heated the gas and stopped BH accretion. Here, $N = 3000$,

and the the GMC has 3000 $M_\odot$ of gas. This gas is fully retained until 1.5 Myr. At that time it is rapidly dispersed, losing the majority of its mass in the next 0.1 Myr.

The maximum stellar mass in each model is a function of the IMF, and is 1.2 $M_\odot$, 10 $M_\odot$, and 30 $M_\odot$, respectively.

The stars and gas in all simulations follow a Plummer distribution. This distribution has a broad central peak, and roughly matches the radial distribution of observed clouds. The initial gas density is taken as

$$\rho_g(r) = 3M_g(0)\ 4\pi r_0^3\ \frac{1}{\left[1+(r/r_0)^2\right]^{(5/2)}} \tag{3}$$

where $M_g(0)$ is the initial gas mass after star formation, r is the distance from the cluster core, and r_0 is a measure of the cluster's radius. The gas mass decays over time, given by

$$M_g(t) = M_g(0) \text{ for t } < \text{ t}_\text{d} \tag{4}$$

$$M_g(t) = \frac{M_g(t=0)}{(t-t_d)\ D} \text{ for t } \geq \text{ t}_\text{d} \tag{5}$$

D is the decay speed, t is the time, and t_d is the the time of the decay start. This dispersion rate is a simple expression used by many simulations with NBODY6.

The positions of individual stars are randomized in three dimensions, following the same distribution envelope as the gas. Initial stellar velocities are set such that the cluster is virialized. No new stars are produced during the runs; however, a few stars are removed as they become gravitationally unbound and evaporate from the cluster. We stop the simulations after 10 Myr for the small cluster, 5 Myr for the medium cluster, and 2 Myr for the large cluster. By these times, the gas has mostly dispersed, and the accretion rate is insignificant.

We checked our simulations for numerical consistency by testing energy and angular momentum conservation. We found the quantities to be properly conserved up until the gas loss began.

4. Results

4.1. Cluster morphology

We first describe the large-scale morphology of our clusters as they evolve.

Figures 1 through 6 show 2D projections of our clusters at their start and end. Several features are apparent. First, the clusters all spread with time. This is due to two effects. First as the gas disperses, the entire cluster expands due to the reduced gravitational potential. In a slow, adiabatic expansion (like our small model) stars are not lost by this process alone, while with a faster dispersion, we expect stars to be ejected. Second, mass segretation occurs, where high mass stars tend to settle toward the cluster center due to dynamical friction and relaxation, allowing low-mass stars (which dominate the cluster in terms of number) to take larger orbits. In our large simulation, we have lost rougly 20% of our stellar mass due to these two effects. The cluster's volume density has decreased by a factor of 10 inward of 0.1 pc, and increased by a factor of 5 outward of 2 pc (Figure 8).

It is instructive to compare our results with previous work. (Kroupa et al. 2001) used the NBODY6 code to model the expansion of the Orion nebula cluster. Using $N = 10^4$ stars, they found that a nearly-instantaneous dispersion of the gas caused the formation of a bound cluster with 30% of the original stellar mass, after XX Myr. They found mass segregation as high-mass stars sank to the core. In a general sense our Large model finds comparable results to theirs. We lose fewer stars, but we almost certainly undertestimate this because we stop our run before stars have time to escape. Furthermore, our gas

dispersion time of 100 kyr is roughly 5x longer than theirs; their faster dispersal time would naturally result in more lost stars due to the non-adiabatic nature of the dispersion. Our results for the evolution of the radial profile are broadly similar to those of Kroupa et al. (2001), with the decreasing in density at the central XX pc, and increasing outward of YY pc.

Our simulations do not consider binaries. We form a handful of short-lived binaries during the runs, but all of them separate within a few timesteps. Realistic modeling of the binary population requires an initial population of binaries; these stars then undergo subsequent three-body interactions to create the final binary population. Our results only apply to single stars. However, for binary stars that are separated by a distance much less than the Bondi-Hoyle radius of ~ 1000 AU, the bulk accretion onto a system should be largely dependent on the total mass of the system, regardless of whether it is a single or multiple star.

4.2. Stellar motions and Bondi-Hoyle accretion

Figures 9 and 10 show the position of stars within the cluster, and their distance from the core. All three of the stars shown have orbit diameters of roughly 0.5 pc. Most stars in the clusters are on eccentric orbits, $e > 0.9$; the Large cluster star shown has a relatively low $e \approx 0.7$. The high eccentricity orbits are characterized by brief passages near the cluster core at < 0.1 pc. Expansion of the cluster is clearly visible for all three stars; the stars' later orbits spread due to the reduced cluster mass. The effect is most noticeable for the Large cluster, where the gas dispersal is the fastest, and least adiabatic. The Large cluster star is on an escaping trajectory and will be lost from the cluster; the other two are retained, but may eventually be lost by the time gas dispersal is complete.

The stellar velocity is plotted in Figure 11. Velocities are lowest in the Small cluster (~ 0.5 km s^{-1}), and highest in the Large (~ 5 km s^{-1}). As the gas disperses, velocities decrease.

Figures 12 and 13 show the BH accretion rate and total accretion amount for the three stars. The accretion rate peaks near the star's periapse, when the stellar velocity is the highest, but the number density is also higher. The integrated mass accretion (Figure 13 increases with time, and is clearly seen to be periodic. By the end of the simulation, the three stars have increased their mass by 3%, 4%, and 2%, respectively.

Figures 14 and 15 show the distribution of mass accretion for all stars in the cluster. The mean accretion rate $\dot{M}_{\rm BH}$ scales as M_*^2, varying across the range 10^{-10} $M_\odot$ yr^{-1} - 10^{-6} $M_\odot$ yr^{-1}. Mass accretion in the large cluster is greater than in the small, but the difference is less than a factor of two.

Accretion in the high-mass stars is significantly higher than lower-mass stars. Most of this difference is due to the dependence of $\dot{M}_{\rm BH}$ on M^2 (eq. 1). The difference in stellar speeds and gas density between high- and low-mass stars makes relatively little difference.

We have computed fits to our data in Figure 14, using a least-squares method in logarithmic space. The results for our three cases are

$$\begin{aligned}
\dot{M}_{\rm BH}({\rm Small}) &\approx 10.0 \times 10^{-9} \left(\frac{M}{M_\odot}\right)^{1.98} M_\odot \ {\rm yr}^{-1} \\
\dot{M}_{\rm BH}({\rm Medium}) &\approx 6.4 \times 10^{-9} \left(\frac{M}{M_\odot}\right)^{2.07} M_\odot \ {\rm yr}^{-1} \\
\dot{M}_{\rm BH}({\rm Large}) &\approx 6.2 \times 10^{-9} \left(\frac{M}{M_\odot}\right)^{2.05} M_\odot \ {\rm yr}^{-1}
\end{aligned} \tag{6}$$

Using a similar method on the data in Figure 15, we compute the total mass accreted for each star. We find that

$$\begin{aligned} dM(\text{Small}) &\approx 0.099 \left(\frac{M}{M_\odot}\right)^{0.98} M_\odot \text{ yr}^{-1} \\ dM(\text{Medium}) &\approx 0.047 \left(\frac{M}{M_\odot}\right)^{1.07} M_\odot \text{ yr}^{-1} \\ dM(\text{Large}) &\approx 0.020 \left(\frac{M}{M_\odot}\right)^{1.05} M_\odot \text{ yr}^{-1} \end{aligned} \tag{7}$$

We would expect the results for $\dot{M}_{\rm BH}$ to cluster around M^2, so out fits are not surprising. Figures 14 shows that or fits are distinctly low for the highest-mass stars. We would expect these stars to have anomalously high accretion rates, because dynamical friction causes them to settle toward the cluster core, where the density is highest. Because there are only a few high-mass stars, our fits are

These fits are to the data shown in figure The large cluster's accretion rate is higher because XXX. The variation between the clusters is only a factor of three; the variation between individual stars of the same mass, in the same cluster, is roughly a factor of 100.

The total mass accreted, for all cases, is

$$dM_{\rm BH} \equiv \int \dot{M}_{\rm BH}\, dt \approx 0.01 \left(\frac{M_*}{M_\odot}\right)^2. \tag{8}$$

The total mass accreted per star (Figure 15) varies by roughly the same factor of 10^2. For solar-mass stars, the median mass accreted is roughly 0.01 $M_\odot$ in both cases. However, in both runs, a few percent of the solar-mass stars accrete between 0.1 $M_\odot$and 1.0 $M_\odot$.

5. Discussion

In this section, we discuss the implications of post-formation accretion. We compare our results with observations, and then propose a bazaar-style multitude of applications of

the process, to formation of our solar system and other planetary systems.

5.1. Observed accretion rates

Recent observations of accretion in young stars has shown that the accretion rate onto the star scales as with the stellar mass: $\dot{M} \sim M_*^2$, with $\dot{M} \simeq 10^{-8}\ M_\odot\ \mathrm{yr}^{-1}$ for solar-mass stars. (The observations cannot distinguish between accretion from the star to the disk, vs. accretion from the molecular cloud onto the disk.) This relationship is apparently robust over the mass range $0.01\ M_\odot - 3\ M_\odot$ (*e.g.* Natta et al. 2006; Muzerolle et al. 2005; Sicilia-Aguilar et al. 2005). There is a large amount of scatter, with values of $\dot{M}$ for comparable values of M_* varying by 10^3 times; the scatter appears to be intrinsic and not observational uncertainty. As counterpoint, (Clarke & Pringle 2006) argues that the $\dot{M} \sim M_*^2$ dependence may be largely an observational effect, due to the fact that the signatures of low accretion rates cannot be detected on top of the fluxes from high-mass stars; in fact, the detectability of accretion also scales with M_*^2.

There is no clear physical reason for the M_*^2 dependence, because the standard models indicate that disk accretion should be independent of disk mass. A recent model by Gregory et al. (2006) improves the standard Gammie layered disk model by assuming a temperature structure that depends on the central star's luminosity. Hartmann et al. (2006) introduces a magnetic field more complex than a dipole; this introduces a mass dependence in the accretion rate. Although these models both move in the correct direction, neither one provides an exponent quite enough to explain the observations. Alexander & Armitage (2006) develops a model that involves photo-evaporation from the central star to speed inner disk evolution. However, this model requires the initial disk's mass to scale as $M_{\mathrm{disk}} \sim M_*^2$, a situation which has not been shown to be true.

Padoan et al. (2005) proposed that the observed luminosity may be due to accretion from the external gas. Indeed, the functional form of BH accretion reproduces the M_*^2 dependence perfectly, and the scatter in the observations could easily be explained by variations in stellar speed, gas density, etc. Their calculations were simple, and only made a single estimate. However, as Hartmann et al. (2006) pointed out, BH accretion depends on the local environment's density and temperature, and the observed $\dot{M}$ values appear to be largely independent of these values. Some stars in HII regions are observed with active accretion up to 10^5 times higher than eq. 1 would predict. In some regions – such as the dark clouds of Taurus – it seems like more than a mere coincidence that BH accretion reproduces both the form of the accretion and its magnitude. In these regions, we believe that BH accretion is probably occurring. There is very little that can stop it! However, in other regions, another process must be at work. It could well be that the accretion is due to several terms, some of which are environmental and some of which depend on the stellar parameters. The large scatter in the data argue for multiple processes. It is not clear if correlations with environment have been made.

The similarity between our results and the observations are striking. The trend, the median, and the scatter are comparable on both. The scatter in our results is a real feature. Furthermore, BH accretion is robust, simple, and solid. As long as the gas remains cool and present, it will occur. For most of the observed stars, this is the case. The regions of Orion Ib, Taurus, XX, XX, etc. are roughly bounded by the parameters of our model.

However, PFA accretion is certainly inhibited in some regions. In particular, regions such as the ONC which contain OB stars do no support PFA, because the gas has already been heated. Heating the gas from 50K to 1000K decreases the gas speed from 1km s^{-1} to 5km s^{-1}, decreasing the nominal accretion rate from 10^{-7} $M_\odot$ yr^{-1} to 5×10^{-10} $M_\odot$ yr^{-1}, for $n = 10^5$ cm^{-3}. This is generally inconsistent with the observations.

Our simulations reproduce the observational result that the observed accretion rate scales as M^2, and is of the order 10^{-8} $M_\odot$ yr^{-1} for solar-mass stars. The accretion rate that we calculate is that onto the star-disk system, not that onto the star. However, assuming the disk serves only as a temporary buffer for material, one would expect $\dot{M}_{\rm BH} \approx \dot{M}_*$.

Although BH accretion can explain some of the observations, it is clear that it can be only a part of the story, because of its strong dependence on the gas density and temperature. Accretion luminosity is seen across a wide range of gas parameters. We stress that we are not solving the $\dot{M} \sim M^2$ problem here. Rather, we are studying the effects of BH accretion on the star and the disk. The accretion rates we compute are entirely consistent with BH accretion being a portion of the observed accretion luminosity.

Our results clearly show that BH mass accretion can be a significant amount. In this section we consider the consequence of the accretion.

FU Orionis outbursts. Bally to fill in here.

5.2. Where does accreted mass go?

The expression for $\dot{M}_{\rm BH}$ expresses, in a general way, the rough amount of material accreting from a medium, onto a compact body. As the flow is focused from the BH radius ($\sim$ 1000 AU) onto the star, it is very likely (depending on orientation) to pass through the exact through the disk. Therefore, the accreting body is not just the star, but the star-disk system.

Many numerical studies have investigated the morphology of the flow pattern (c.f. Edgar 2004, and references therein). The most relevant of these include to the parameter space we study are those of Ruffert (1999, 1997); Benensohn et al. (1997). These hydrodynamic simulations modeled the accretion of material at $v/c \sim 3 - 10$, comparable to the range

we use. They included small gradients of velocity and density in the background gas, and modeled the central accretor as a finite, stellar-sized body. They found the resulting accretion to be not a steady flow, but dominated instead by a 'flip-flop instability.' The accretion was not a steady flow onto the body, but instead set up a temporal, tenuous disk surrounding the star, at a distance of 1-200 AU. The disk oscillated between prograde and retrograde motion as it served as a temporary buffer for material before it was accreted onto the star. The instability caused a variability in accretion rate $\dot{M}_{\rm BH}$ of 2-10x on keplerian timescales. The disk's density was $\sim 10^{-3}$ that of a MMSN disk (*e.g.* Hayashi 1981). They found that the majority of the mass and angular momentum within the accretion radius ($R_{\rm BH}$) was ultimately accreted onto the star.

It seems clear from simulations that the BH flow will almost certainly interact with an existing disk. Over a time period of several Myr, the amount of accreting mass passing through the disk is on the order of a disk mass (for a MMSN). The nature of the interaction is unclear, but likely involves mass transport through the disk, which is ultimately delivered to the star. (It is unlikely that accretion will miss the disk; observations indicate that it is also unlikely that the disk will *not* deliver mass to the star.)

Simulations of this process have not been done. It is not clear under what circumstances the disk's lifetime may be shortened, or extended. This may depend on the nature of the gradients (and turbulence) within the molecular cloud.

Effect on planets. Planetary cores and gas-giant planets are often thought to form on timescales of 5-15 Myr (). This is toward the later end of our calculations, but it is instructive to see if accretion onto these bodies could be important. Keplerian speeds for the gas giants and planetesimals at 5-50 AU from a 1 $M_\odot$ star are 13 km s^{-1} - 4 km s^{-1}, respectively. At the inner edge

A simple application of eq. [1]

Because the accretion flow is 10^3x weaker than the disk, it is unlikely that substantial material from the flow will accrete onto planets. However, gas could fill up depleted 'feeding zones' in the disk.

Effect on the star. We find the accretion of material onto the central star raises its mass by

For solar-mass stars, the 1% increase in mass has insignificant dynamical effect. However, for higher-mass stars, if the composition of the infall material differs from that of the star, then an insignificant amount of mass may make a substantial difference in the observed stellar metallicity. The magnitude of this effect depends on the size of the star's convective envelope. For solar-mass stars in their first 10 Myr, the stars are essentially fully convective, meaning that additional material dumped onto their surface will be fully-mixed. Higher-mass stars are fully convective at the star, but soon evolve so that only their thin out veneers are convective. For instance, stars of 2.5 $M_{\odot}$at 2 Myr are approximately 10% convective (Laughlin & Adams 1997). Thus, the effect of a small amount of 'foreign' material is effectively amplified by ten times. This process has been modeled by Laughlin & Adams (1997) to describe the change in observed metallicity of a star after it has absorbed rocky material from young planets spiraling onto the star.

In our case, invoking this effect requires a spatial compositional difference in the raw material of the parent molecular cloud. Such a variation could occur in GMCs based on the cloud's history – for instance, material ejected from a nearby supernova could mix with homogeneous molecular material. Such a scenario could be possible in the Orion region, where supernova remnants and active star-forming regions co-exist.

Work by Cunha et al. (1998, 1995) has investigated precisely this possibility in Orion. They studied the metallicity of approximately 20 F, G, and B stars in Orion. They found spatial variations of composition which varied by a factor of 4 (0.6 dex), even within the

same Orion Ic association. Most compellingly, they found that the abundance of Fe, C, and N was best-represented by a single value, while the abundance of O and Si was best-fit by a range of values. Because O and Si are produced much more readily by massive stars (including supernovae) than is Fe, they hypothesized that portions of the molecular cloud were polluted by massive stars, and subsequent accretion of material reflects this variation.

The abundance variations could be caused by accretion at the time of star formation, or post-formation. The large variation suggests it may have happened post-formation when, because of their smaller convective zones, the stars are more susceptible to 'pollution.'

The highest mass stars in our study have the highest accretion rate as a fraction of their mass. In fact, 30% of the stars in the $5 - 10\ M_{\odot}$ range accreted over $5\ M_{\odot}$. This is probably unrealistic, for two reasons. First, our model is not self-consistent, in that the gas cloud's total mass is reduced globally, but not locally. The high mass stars congregate at the cluster core, where the stellar density is the highest, and thus gas is depleted first. Second, stellar winds from high-mass stars ($> 10\ M_{\odot}$) can begin to inhibit BH accretion. Additional work by Bonnell et al. (2001) looks into the effect of post-formational accretion on the cluster IMF.

Regardless, *some* stars in both of our runs accrete a significant fraction of their mass. For these stars, an increase in stellar mass would have an unusual effect on an accompanying circumstellar disk. Assuming mass is accreted slowly (adiabatically), the disk's dimensions will shrink. For an increase in mass of 2x, conservation of angular momentum shows that the the orbital distance of any material will decrease by the same factor, turning (for instance) a 50 AU disk into a 25 AU one. This could be a way to bring icy material inward of the snow line, or migrate giant planets inward without invoking a drag force.

Effect on gas giant planets. If pollution by spatial variations across the gas cloud are indeed responsible for these stars' abundance variations, then we must ask what the

effect on abundances in the disk and its planets could be. Modeling of the interaction between the inflow and planets has not been done, but the fraction of 'foreign' material incorporated into a growing planet would likely be a complex function of the particular flow, disk, and planet parameters. In some cases a planet could incorporate very little of the inflow material, and in others, perhaps a substantial amount could be incorporated. Detailed modeling is probably unimportant at this early point of the understanding of the process. However, it seems reasonable that differential rates of accretion and convection between planets and stars could yield significantly different values for their observed final abundances.

Laughlin & Adams (1997) investigated the effect of infalling planets (or planetesimals) on to a star. This would increasing a star's metallicity relative to that of its planets. Post-formation accretion could have the same effect. The process could lead to either an enhancement or reduction in a star's metallicity – *e.g.*, a thin veneer of 'dirty' material on top of a 'clean' 2.5 $M_{\odot}$ star could mask such a star's interior. The total amount of 'foreign' material falling onto a star in our studies exceeds that of a planet falling onto the surface; our median value of 0.01 $M_{\odot}$ is equal to 10 Jovian masses. Laughlin & Adams (1997) found an appreciable effect with infall of just one Jupiter, so our effect could be much bigger than that.

In our own solar system, Jupiter is enhanced by $3 - 10x$ over the Sun in most metals (*e.g.* Atreya et al. 2003). Uranus and Neptune are enhanced by greater fractions. This is suggestive of the Sun accreting a layer of 'clean' material. Such a veneer would be expected to be accreted less by Uranus and Neptune, because of their lower mass and the M^2 dependence of the BH accretion rate. Because the Sun's convective zone covers roughly a third of its mass, lowering the Sun's abundance sufficiently requires accretion of substantial amounts of material, on the order of 0.1-0.2 $M_{\odot}$. Several percent of the solar-mass stars in

our study indeed do gain this much. However, this is admittedly greater than the median value of 0.01 $M_{\odot}$, so such a scenario may be statistically unlikely.

Effect of angular momentum. If the background medium is entirely free of velocity and density gradients, then no angular momentum is transferred to the accretor. Real molecular clouds are rarely this idealized. This can be seen by the common existence of disks surrounding stars: in the collapse into the initial protostar, the majority of *mass* falls to the center, while the majority of the *angular momentum* is given to the disk. Numerical simulations by Ruffert (1999) investigated the accretion of angular momentum onto a star. They found that while the accretion efficiency for mass within the accretion radius was very close to 100%, the accretion efficiency for angular momentum ranged from 3% to 70%. The highest efficiencies corresponded to models with the highest density gradients. All of these values may be somewhat high for our case, because Ruffert (1999) used an accretor which was (due to necessary resolution issues) only several times smaller than the accretion column. In the astrophysical case the accretor will be much smaller, causing a decrease in angular momentum actually accreted.

Observed accretion rates (eg gullbring): signature from accdisk and accbh are indistinguishable. Gullbring assumes 5 rsun, but energy level for that is essentially same as from infinity.

Even a small amount of accretion can lead to a large increase in a star's observed metallicity.

Could explain tilt of the Sun. (eg blt97)

Q: How much 'enhanced' gas would it take for the Sun to be enhanced (or depleted) relative to Jupiter or other stars? Look in Laughlin + Adams paper?

Effect of gas on formation of solar system. Many models for the formation of

the solar system have difficult explaining the low eccentricity of the terrestrial planets. In order to collisionally grow, planetesimals in the terrestrial planet zone require high eccentricities. Their present-day low eccentricities ($e \sim 0.001$) cannot easily be explained without a damping mechanism. Agnor & Ward (2002) suggested that the eccentricities could be damped by a relatively long-lived remnant gas disk. They computed that a disk of surface density $\sim 10^{-3} - 10^{-4}$ that of the MMSN, and surviving for $10^6 - 10^7$ years, would provide the necessary damping mechanism.

The simulations of PFA by Ruffert (1999) produced a disk with roughly 10^{-3} the surface density of the MMSN. Such a turbulent, unstable disk is likely to be transient and disperse soon after its supply of gas is cut off. (Ruffert's disk was transient, and such a disk when superimposed onto an existing planetary disk would probably be even shorter lived.) Gas in a molecular cloud can be cut off within 10^4 yr in response to a supernova, which could easily be triggered several Myr after the disk is formed. Therefore, PFA model could plausibly provide the requirements on a damping gas disk required to explain the terrestrial planets' circular orbits.

Halting migration of planets. In much the same way that a long-lived gas disk could circularize planetary orbits, drag by such a disk could also cause their radial migration. Many planetary systems have been found very close to their host stars, suggesting that they migrated inward from regions of higher density where they were formed. Migration could be caused by a gas disk; however, such a disk requires a rapid dispersal mechanism in order to halt the migration. Photo-evaporation by the central star (Matsuyama et al. 2003) has been proposed as one such mechanism.

We note that the PFA scenario also could cause such a setup. Inward migration of planets and/or planetesimals would be caused by a tenuous gas disk. At the time of a supernova, such a disk would rapidly disperse as its source from the molecular cloud is

heated and/or removed.

5.3. Effects of simplifying assumptions

Gas turbulence. We have assumed a uniform, laminar flow of material in the BH flow. In reality, the gas medium will have turbulence and shear, and the local variations in the velocity field will affect the accretion flow. For instance, if a star passes through a portion of the cloud with shear, the resulting flow asymmetry may need to be considered. Work by Ruffert (1997) and Livio et al. (1986) has addressed this issue. Both works used SPH simulations to model the accretion flow from a turbulent and/or shearing medium, onto a finite-sized observer. Ultimately, all of the studies found that within a factor of 2, the simple expression of 1 do an excellent job of describing the flow rate. However, they emphasize that the accretion rate is that onto a star-disk system. Work by Ruffert (1997) modeled the accretion from a shear flow. He found that the accretion flow created many transient accretionary features around the star. The most dramatic of these was an oscillatory prograde-retrograde disk surrounding the star. The disk had a mass of XX and radius of YY. Ruffert (1997) did not include a pre-existing disk in their calculations, so it is not clear if such a disk would form in the presence of a (relatively) massive existing disk. However, it is compelling

6. Conclusions

In this paper, we have studied the accretion of molecular gas onto young star-disk systems. We investigate this process's consequence on stars, disks and pre-planetary systems. We find the following conclusions:

- Post-formation accretion (PFA) can occur in the majority of stars in both cool clouds like Taurus, and large clouds like Orion: in the former, the process may be active for XX Myr, while in the latter, the process is truncated after several Myr when the GMC is ionized due to the birth of massive stars.

- Typical accretion rates for solar-mass stars are 10^8 $M_\odot$ yr^{-1}. The accretion rate scales with the square of the stellar mass, $\dot{M} \sim M_*^2$.

- Approximately 1% of star-disk systems double their mass by accretion.

- There is a scatter of roughly 100x between the highest and lowest accretion rates for a given stellar mass. This scatter is caused by variations in density and velocity as individual stars orbit a cluster.

- A typical solar-mass star received 0.01 $M_\odot$of material accreted onto its star-disk system. This mass is equal to a minimum-mass solar nebula (MMSN), and most of the material probably is processed through the disk, rather than accreting onto the star directly.

- Processing this much material through the disk over the first several Myr may have substantial impact on the disk's dynamics and the formation of planets, but these effects are unexplored.

- Post-formation accretion could supply a long-lived, tenuous gas disk until after the formation of planets, which is removed after a supernova event. Such a disk could explain the low eccentricity of the Sun's terrestrial planets, and the inward radial migration of extrasolar planets.

- Variations in elemental abundances or gas:dust ratios across a molecular cloud are sufficient to explain a metallicity difference between planets, and their host stars.

Either one could be depleted (or enhanced), but the process may be easiest for $M_* > 2\ M_\odot$, where the star's convective fraction is small.

7. Acknowledgments

We are grateful to Sverre Aarseth for providing his NBODY6 code and providing us with enthusiastic support. This work has benefited from discussions with many of our colleagues, in particular Hal Levison, Martin Duncan, and David Devine.

REFERENCES

Aarseth, S. J. 1999, PASP, 111, 1333

Adams, F. C., Proszkow, E. M., Fatuzzo, M., & Myers, P. C. 2006, ApJ, 641, 504

Agnor, C. B. & Ward, W. R. 2002, ApJ, 567, 579

Alexander, R. D. & Armitage, P. J. 2006, ApJ, 639, L83

Atreya, S. K., Mahaffy, P. R., Niemann, H. B., Wong, M. H., & Owen, T. C. 2003, Planet. Space Sci., 51, 105

Bally, J., Sutherland, R. S., Devine, D., & Johnstone, D. 1998, AJ, 116, 293

Bate, M. R. & Bonnell, I. A. 2005, MNRAS, 356, 1201

Benensohn, J. S., Lamb, D. Q., & Tam, R. E. 1997, ApJ, 478, 723

Bondi, H. 1952, MNRAS, 112, 195

Bondi, H. & Hoyle, F. 1944, MNRAS, 104, 273

Bonnell, I. A., Clarke, C. J., Bate, M. R., & Pringle, J. E. 2001, MNRAS, 324, 573

Clarke, C. J. & Pringle, J. E. 2006, MNRAS, 370, L10

Cunha, K., Smith, V. V., & Lambert, D. L. 1995, ApJ, 452, 634

—. 1998, ApJ, 493, 195

Edgar, R. 2004, New Astronomy Reviews, 48, 843

Gregory, S. G., Jardine, M., Simpson, I., & Donati, J. F. 2006, MNRAS, 371, 999

Hartmann, L., D'Alessio, P., Calvet, N., & Muzerolle, J. 2006, ApJ, 648, 484

Hayashi, C. 1981, Progr. Theor. Phys. Suppl., 70, 35

Hillenbrand, L. A. 1997, AJ, 113, 1733

Kroupa, P., Aarseth, S., & Hurley, J. 2001, MNRAS, 321, 699

Kroupa, P., Tout, C. A., & Gilmore, G. 1993, MNRAS, 262, 545

Krumholz, M. R., McKee, C. F., & Klein, R. I. 2006, ApJ, 638, 369

Laughlin, G. & Adams, F. C. 1997, ApJ, 491, L51

Livio, M., Soker, N., de Kool, M., & Savonije, G. J. 1986, MNRAS, 222, 235

Matsuyama, I., Johnstone, D., & Murray, N. 2003, ApJ, 585, L143

Muzerolle, J., Luhman, K. L., Briceno, C., Hartmann, L., & Calvet, N. 2005, ApJ, 625, 906

Natta, A., Testi, L., & Randich, S. 2006, A&A, 452, 245

Padoan, P., Kritsuk, A., Norman, M., & Nordlund, A. 2005, ApJ, 622, L61

Ruffert, M. 1997, A&A, 317, 793

—. 1999, A&A, 346, 861

Sicilia-Aguilar, A., Hartmann, L. W., Hernandez, J., Briceno, C., & Calvet, N. 2005, AJ, 130, 188

Parameter	**Small**	**Medium**	**Large**
N	30	500	3000
$M_{\rm gas}$	30 $M_\odot$	500 $M_\odot$	3000 $M_\odot$
Half-mass radius, stellar	0.2 pc	0.2 pc	0.2 pc
Half-mass radius, gas	0.2 pc	0.2 pc	0.2 pc
SFE	33%	33%	33%
Central stellar density (N pc^{-3})	6×10^2	10^4	10^5
Central gas density (n cm^{-3})	2×10^4	4×10^5	2×10^5
Stellar mass range	0.1 - 1.2 $M_\odot$	0.1 - 18 $M_\odot$	0.1 - 27 $M_\odot$
Mean stellar mass	0.5 $M_\odot$	0.5 $M_\odot$	0.5 $M_\odot$
Gas dispersal delay time	5 Myr	3 Myr	1.5 Myr
End time	10 Myr	4.85 Myr	2 Myr

Table 1: Initial conditions for three stellar cluster models.

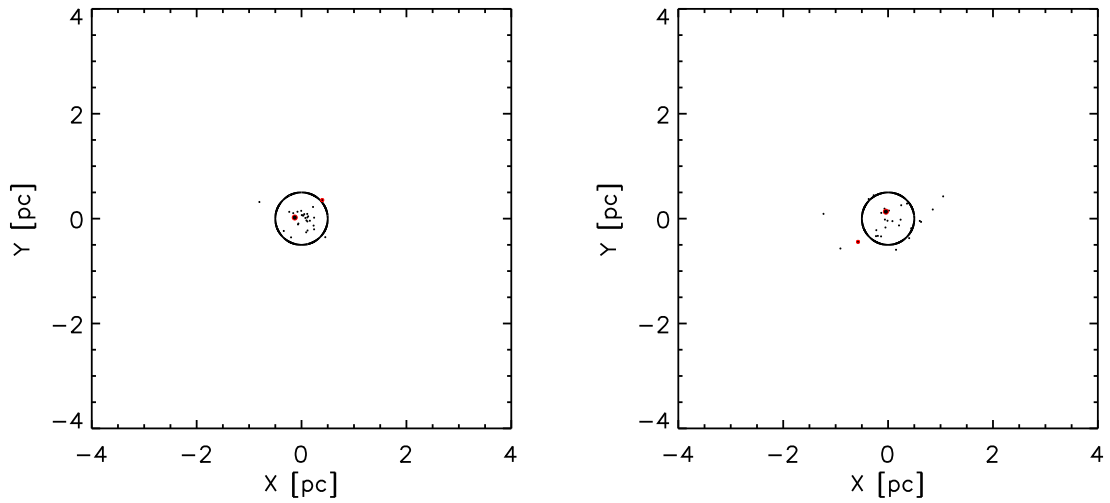

Fig. 1.— Cluster view, Small, start and end.

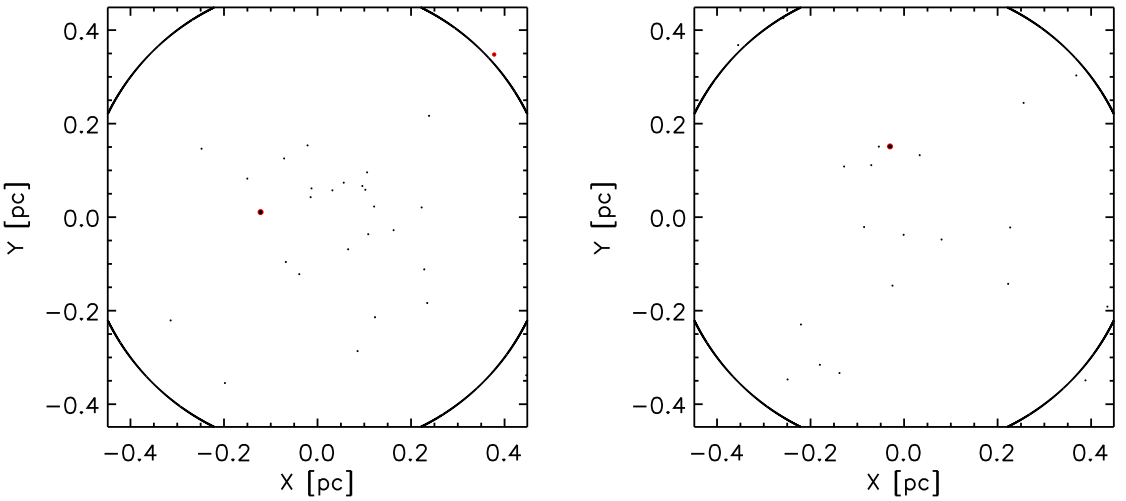

Fig. 2.— Cluster view, Small, start and end, core.

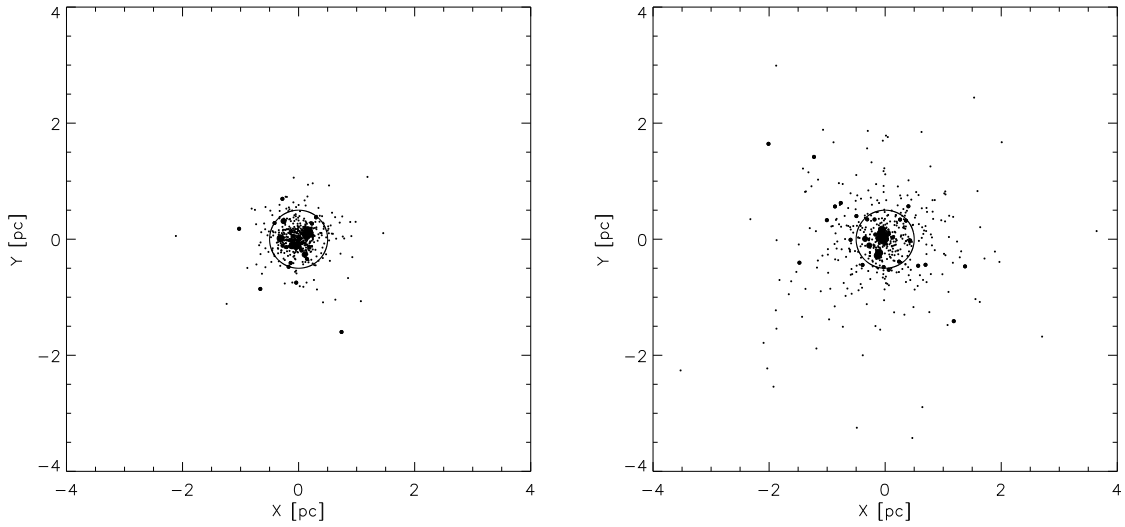

Fig. 3.— Cluster view, Medium, start and end.

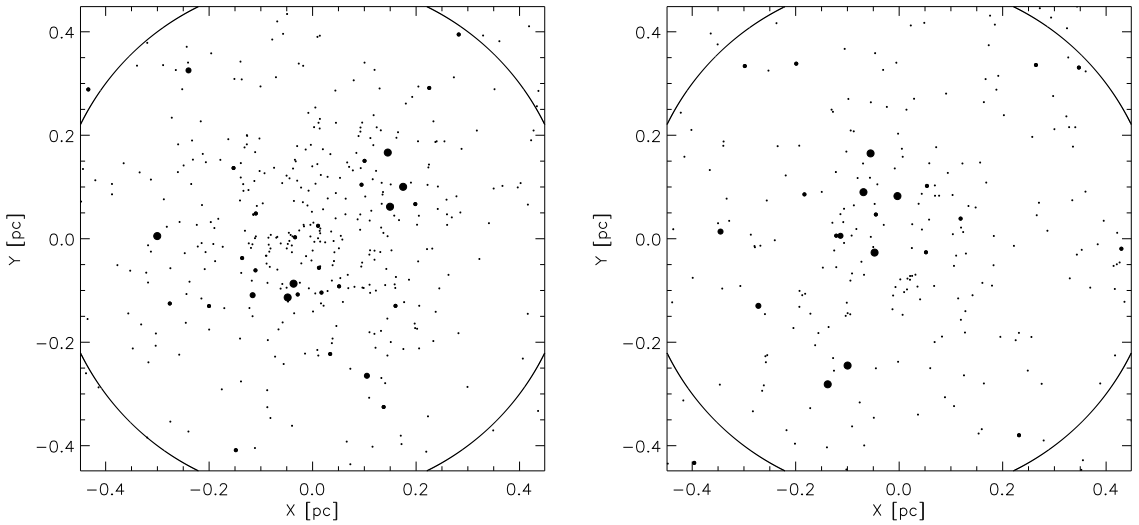

Fig. 4.— Cluster view, Medium, start and end, core.

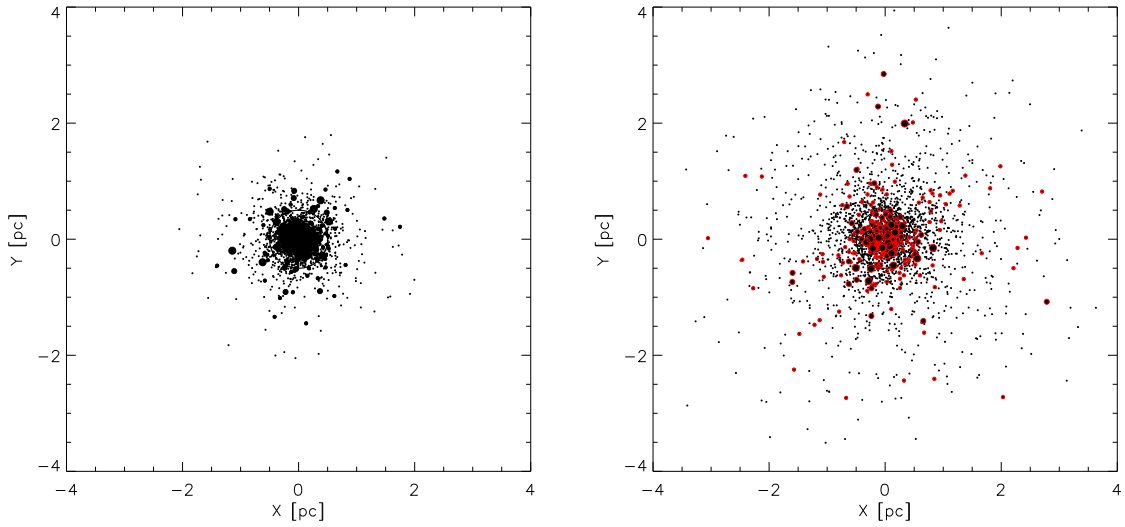

Fig. 5.— Cluster view, Large, start and end.

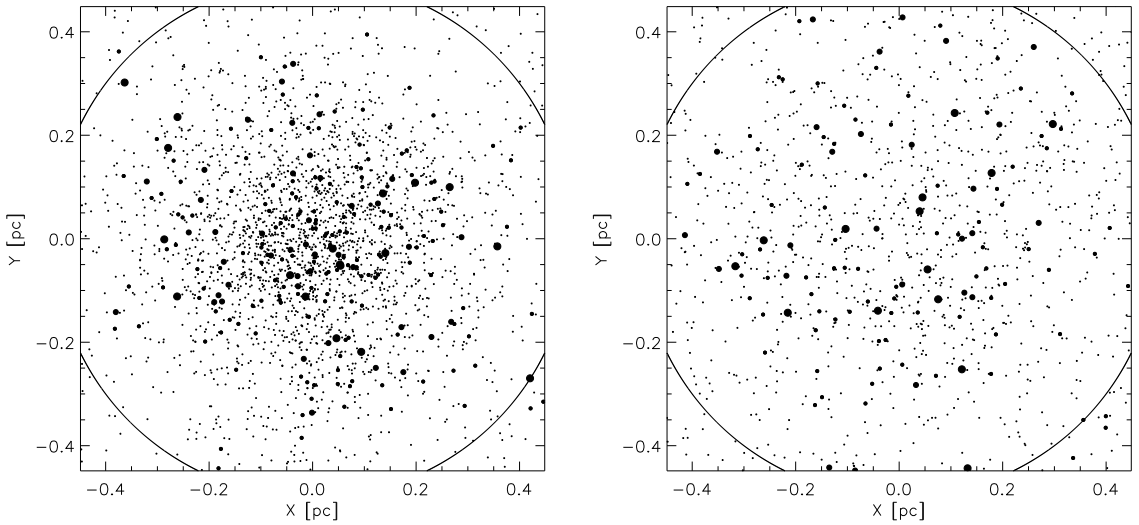

Fig. 6.— Cluster view, Large, start and end, core.

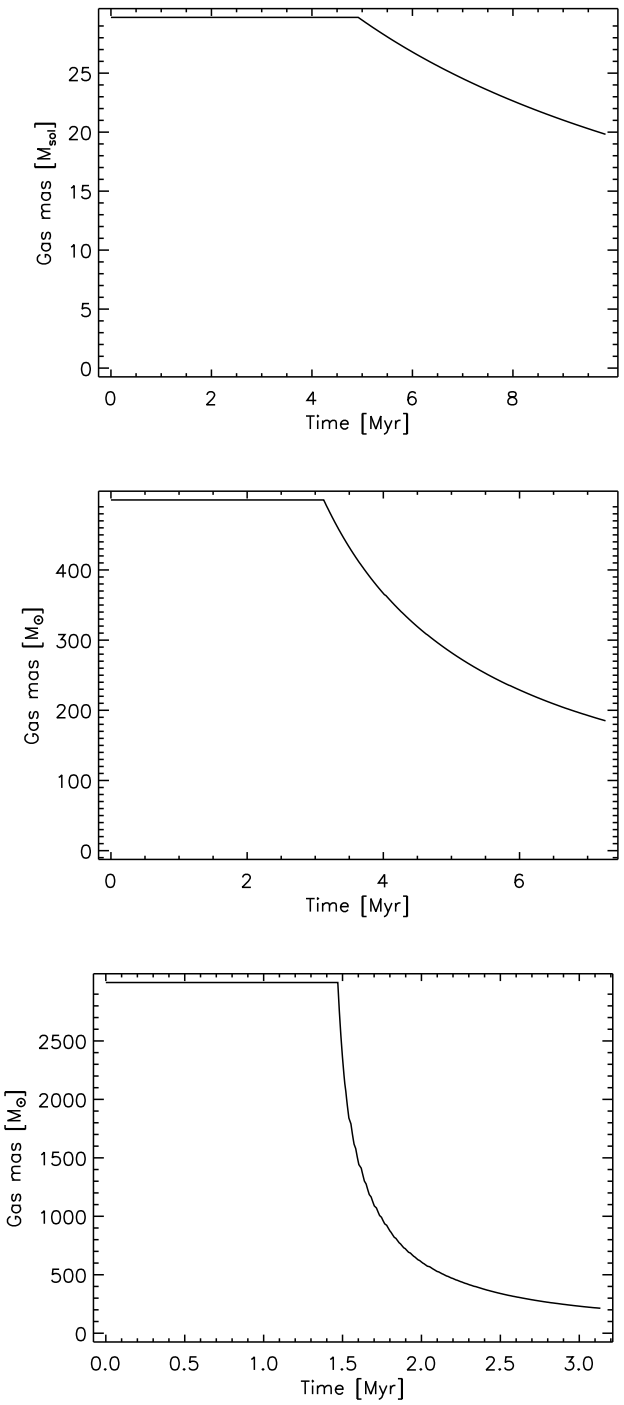

Fig. 7.— Gas masses in each cluster as a function of time. **A**: Gas dispersion for the Small cluster. **B**: Gas dispersion for our Medium cluster. The gas is fully retained until 3.5 Myr, at which point it begins to slowly disperse. **B**: Gas dispersion for our Large cluster. In this case, the gas disperses quickly at 1.5 Myr, simulating the onset of massive star formation.

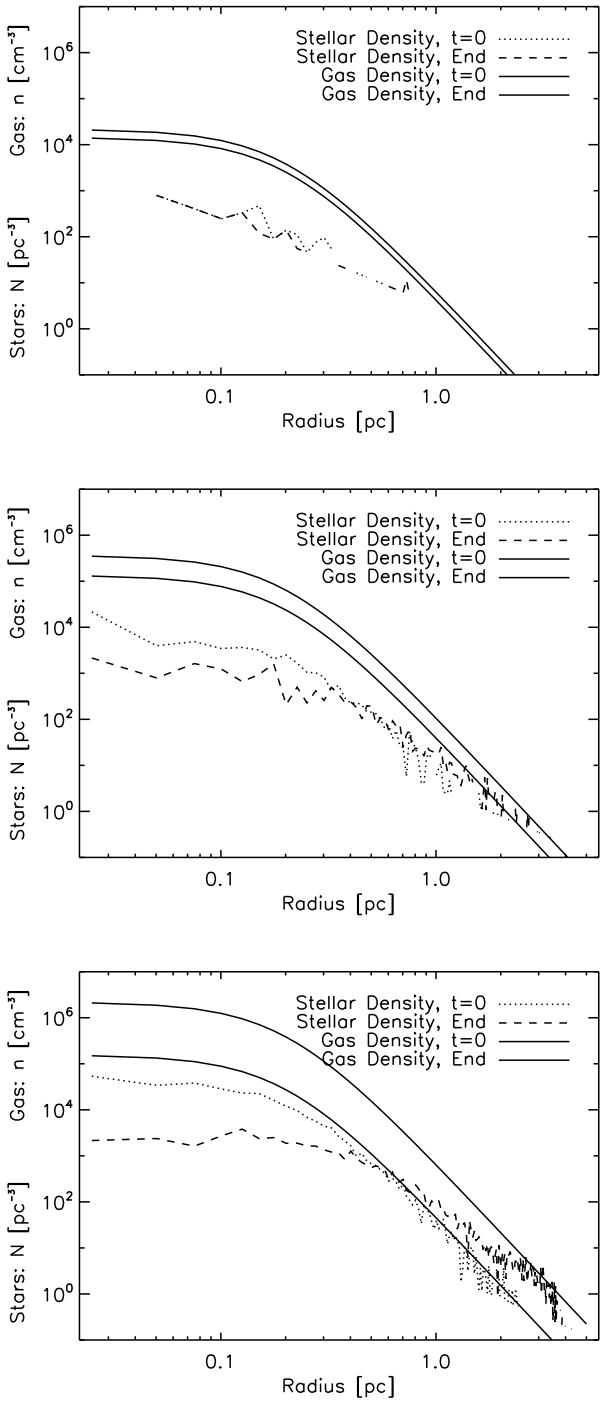

Fig. 8.— Radial distribution of material for our three clusters. The gas density and stellar density are shown on the same axis. The spreading of the Medium clusters as their gas disperses is clear. The Small cluster's spreading is more difficult to see, due both to less spreading, and statistics with its fewer stars.

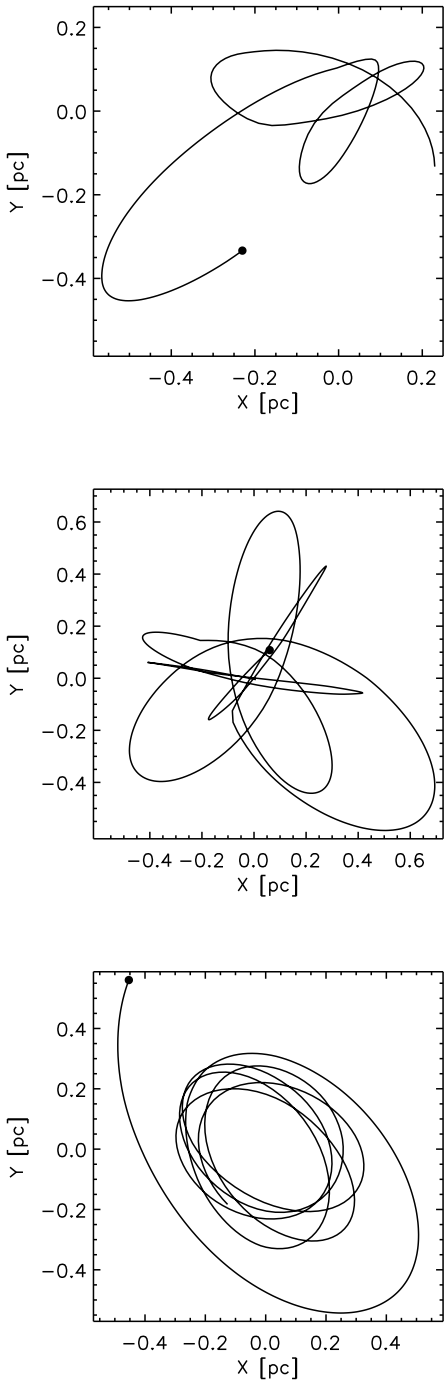

Fig. 9.— Stellar position for three sample stars, taken from the Small, Medium, and Large simulations. Stellar masses are 0.53 $M_{\odot}$, 1.1 $M_{\odot}$, and 1.8 $M_{\odot}$, respectively. Each star's final position is shown with a filled circle.

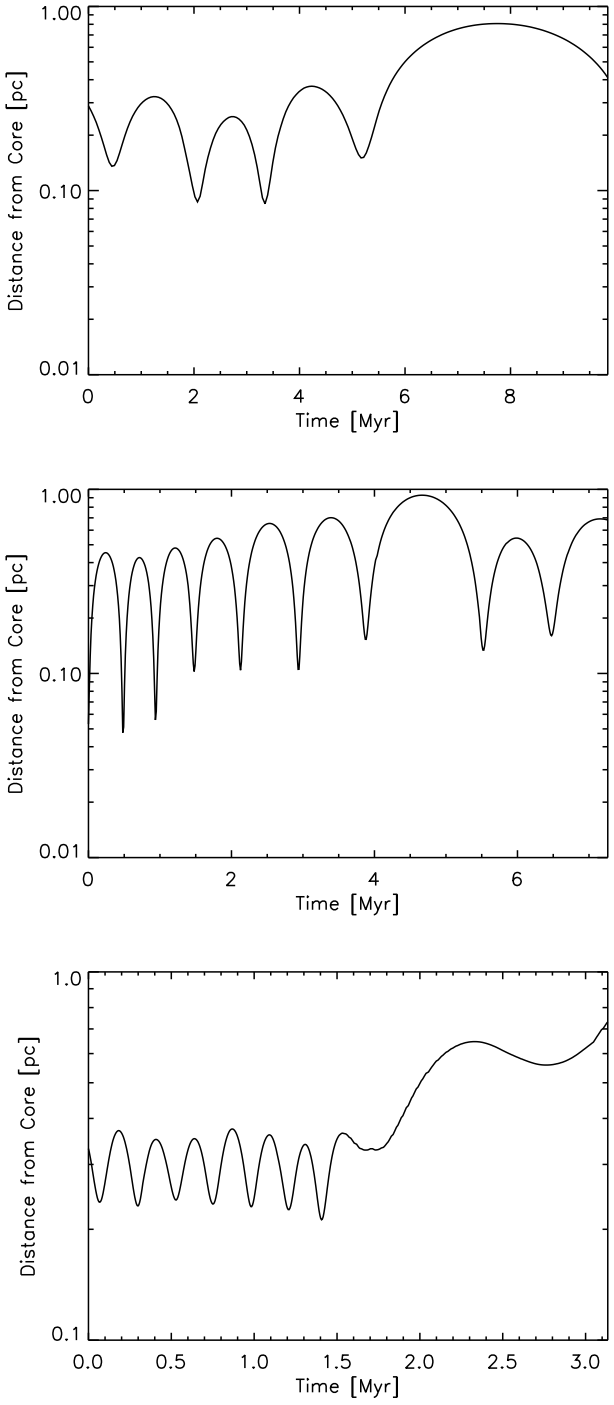

Fig. 10.— Stellar distance from core. Stars are the same as identified in Figure 9.

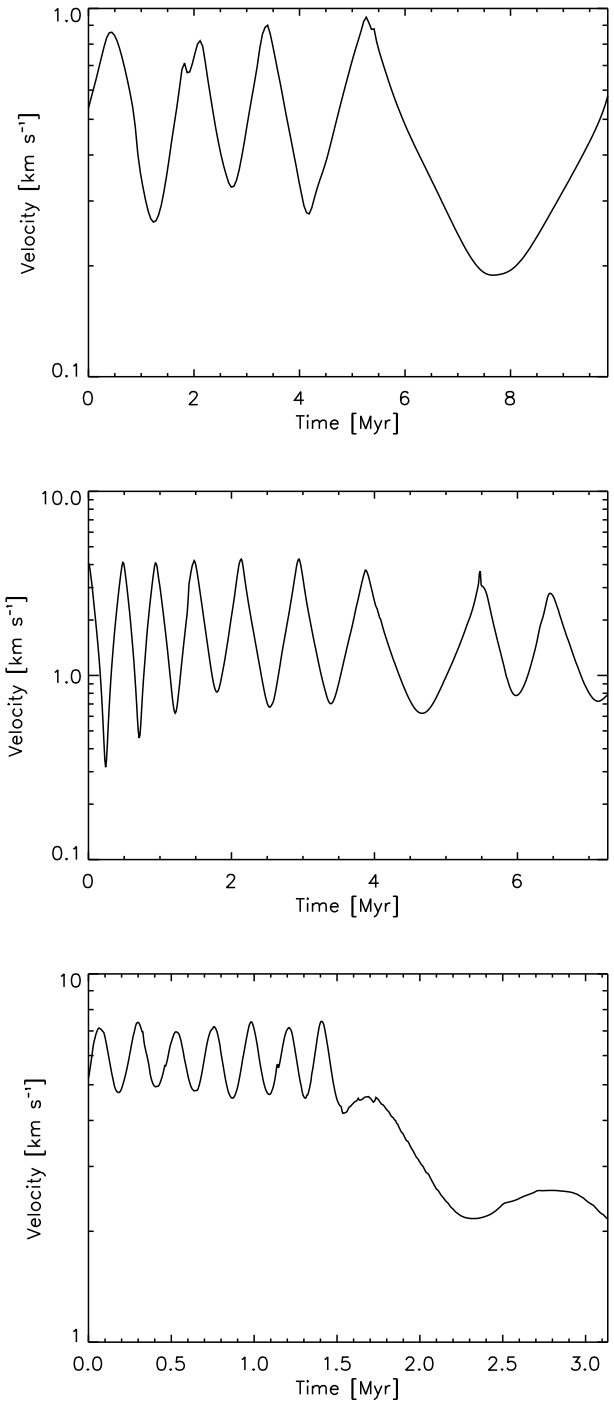

Fig. 11.— Stellar velocity. Stars are the same as identified in Figure 9.

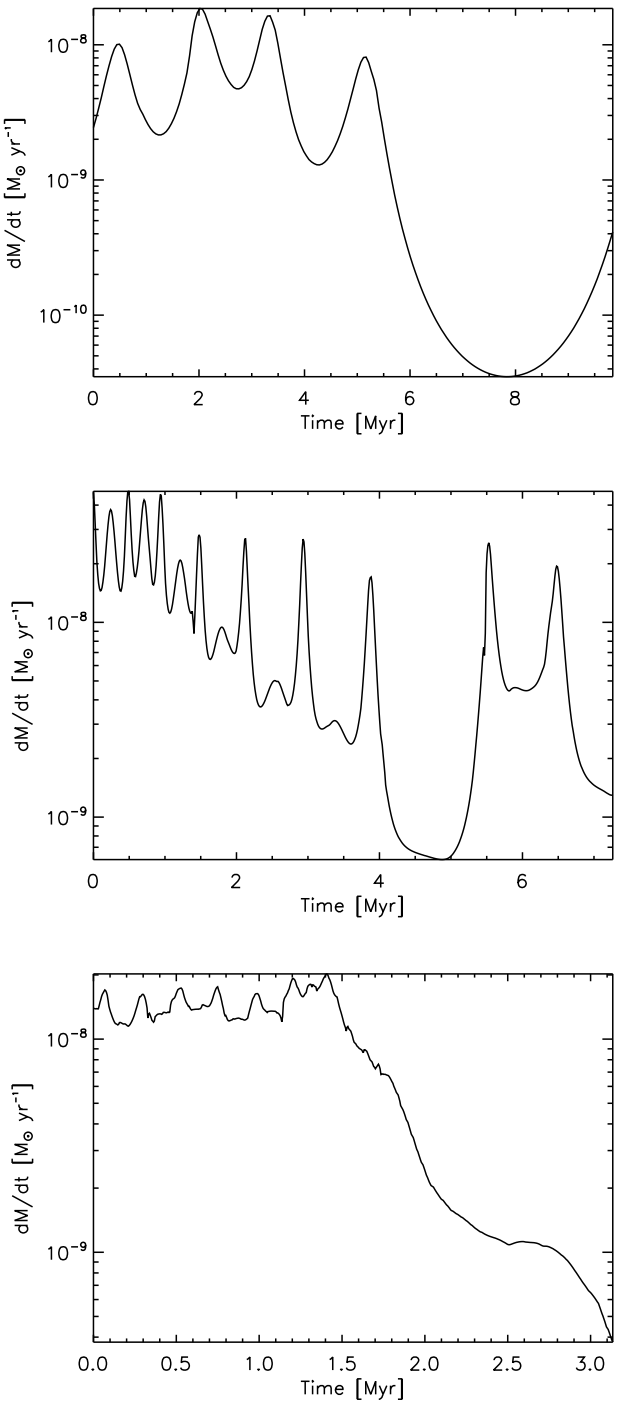

Fig. 12.— BH accretion rate, $\dot{M}_{\rm BH}$. Stars are the same as identified in Figure 9.

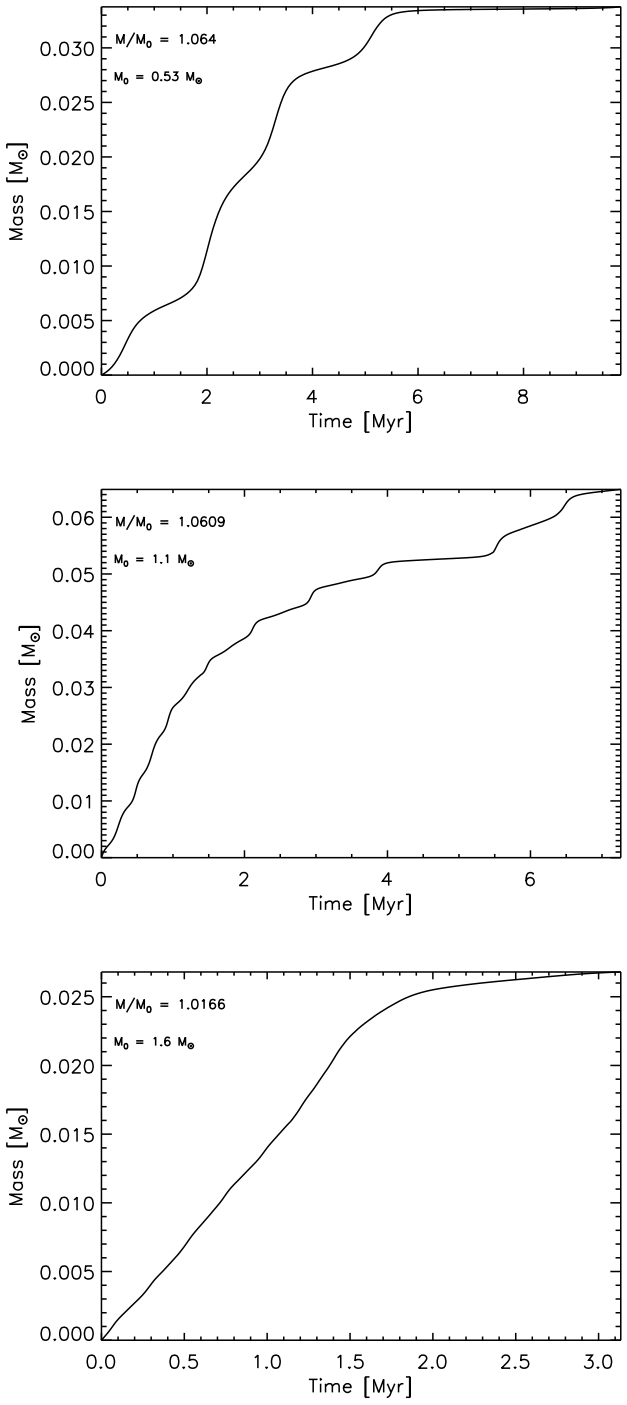

Fig. 13.— BH total accretion amount, $\int \dot{M}_{\rm BH}\ dt$. Stars are the same as identified in Figure 9.

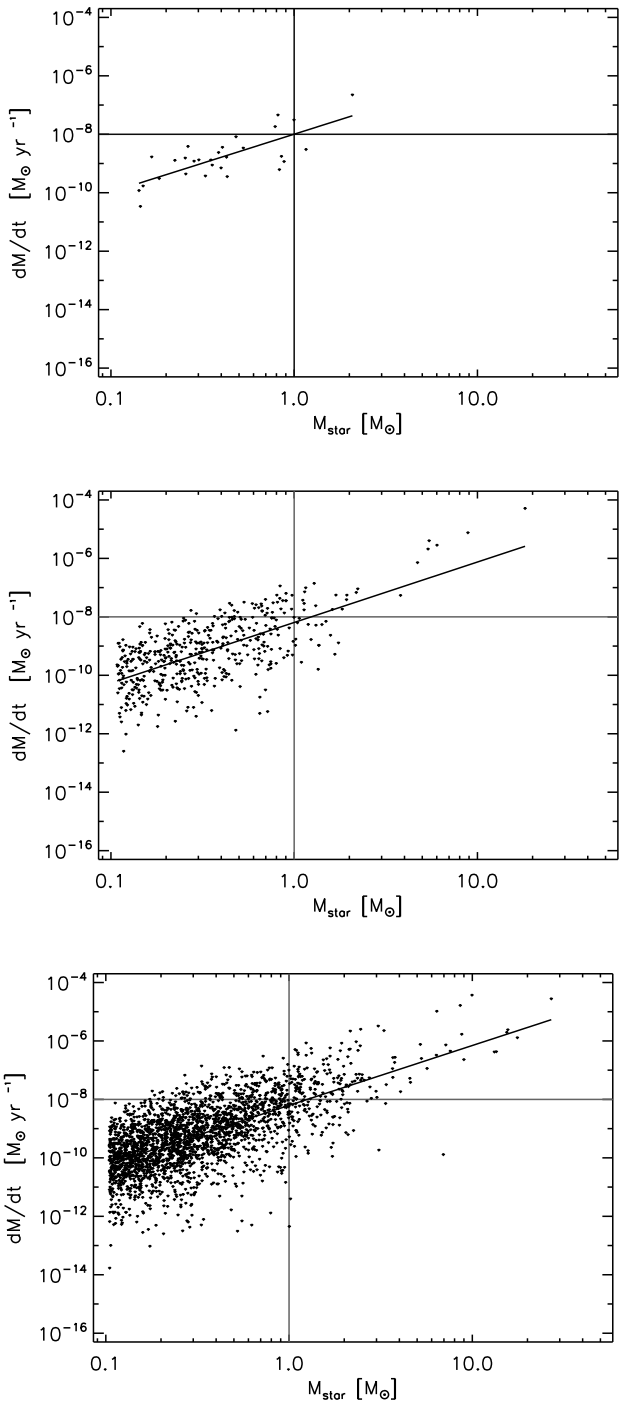

Fig. 14.— Mean $\dot{M}_{\rm BH}$ for the Small, Medium, and Large clusters. Each point corresponds to one star in the simulation. The solid lines are show the median mass accretion rate, binned by mass.

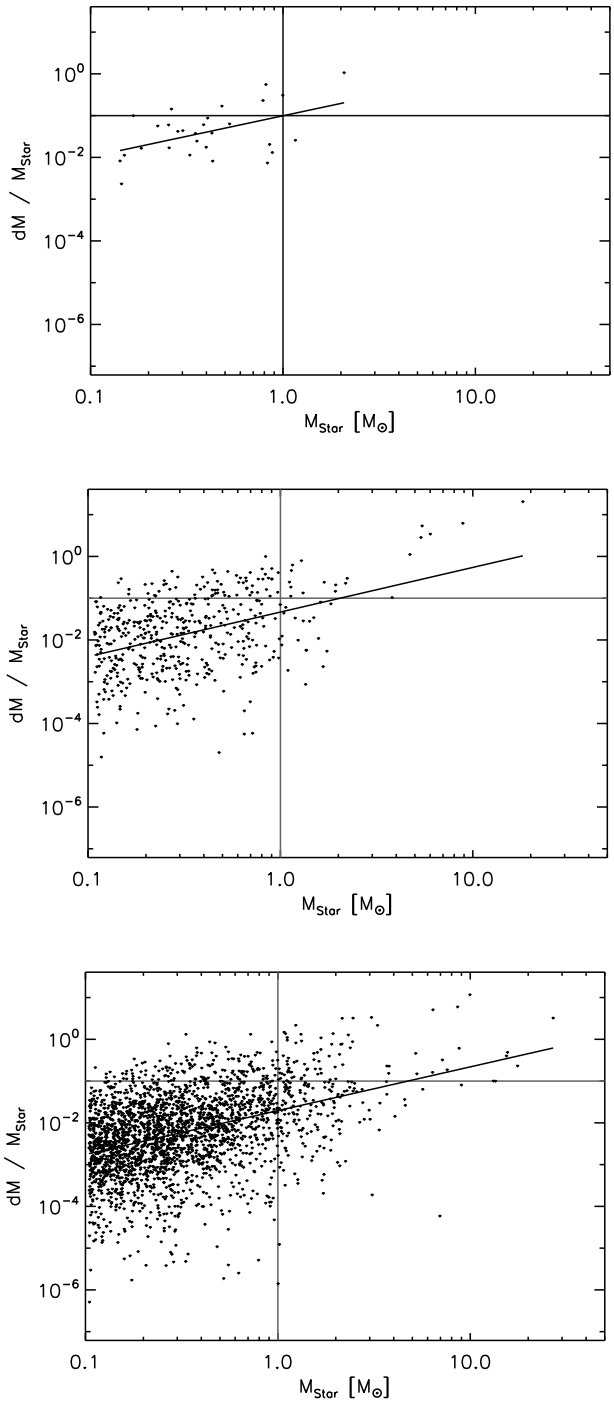

Fig. 15.— Total mass growth, $\int \dot{M}_{\rm BH}\, dt$. Each point corresponds to one star in the simulation. The solid lines show the median mass accretion rate, binned by mass.

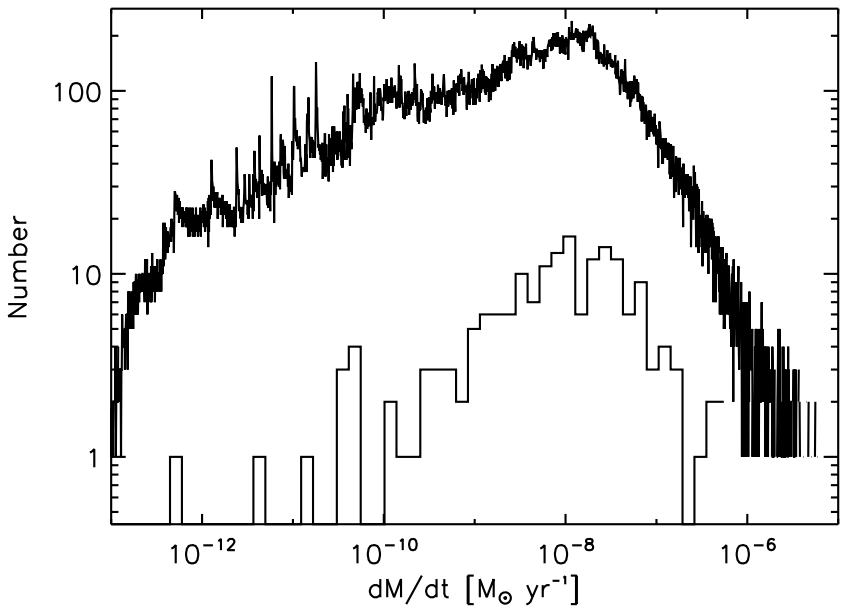

Fig. 16.— Spread in $\dot{M}_{\rm BH}$, for solar-mass stars in the Large cluster. The top curve shows the range of values of $\dot{M}_{\rm BH}$ for the entire simulation, with one data point per star, per timestep. The lower curve uses only the mean values of $\dot{M}_{\rm BH}$, not the instantaneous values. Thus, the spread in the lower curve is due to variation in stars' initial conditions, while the spread in the upper curve also includes time-variability of accretion during an orbit. Stars have masses 0.8 - 1.2 $M_\odot$; this range of mass does not significantly widen the plot.